# Chemical vapor deposition of $HfO_2$ films on Si(100)

S. Sayan
*Department of Chemistry, Rutgers University, Piscataway, New Jersey 08854*

S. Aravamudhan
*Department of Chemistry, Rutgers University, Piscataway, New Jersey 08854 and Agere Systems, Electronic Device Research Laboratory, Murray Hill, New Jersey 07974*

B. W. Busch
*Department of Physics and Astronomy, Rutgers University, Piscataway, New Jersey 08854 and Agere Systems, Electronic Device Research Laboratory, Murray Hill, New Jersey 07974*

W. H. Schulte
*Department of Physics and Astronomy, Rutgers University, Piscataway, New Jersey 08854*

F. Cosandey
*Department of Ceramics and Materials Engineering, Rutgers University, Piscataway, New Jersey 08854*

G. D. Wilk
*Agere Systems, Electronic Device Research Laboratory, Murray Hill, New Jersey 07974*

T. Gustafsson
*Department of Physics and Astronomy, Rutgers University, Piscataway, New Jersey 08854*

E. Garfunkel[a)]
*Department of Chemistry, Rutgers University, Piscataway, New Jersey 08854*

(Received 19 September 2001; accepted 17 December 2001)

$HfO_2$ films were grown on Si(100) by chemical vapor deposition as an attempt to develop an industrially straightforward gate dielectric deposition process. During deposition at $\sim 400\,^{\circ}C$ the decomposition of the hafnium-tetra-tert-butoxide $Hf(C_4H_9O)_4$ precursor provides sufficient oxygen to produce a stoichiometric $HfO_2$ film. Medium energy ion scattering, high resolution transmission electron microscopy, atomic force microscopy, and ellipsometry were used to identify the structure and composition of the film and its interface to the Si substrate. Local crystallinity in the films increased significantly with annealing. Capacitance–voltage and current–voltage methods were used to characterize the electrical properties of simple capacitor structures. When grown on high quality ultrathin oxides or oxynitrides, the deposited films displayed very good physical and electrical properties. © *2002 American Vacuum Society.* [DOI: 10.1116/1.1450584]

## I. INTRODUCTION

The continuous scaling of semiconductor devices to achieve higher speed, density, and computational ability at lower power consumption and cost has been maintained for more than 30 years. One critical component, the gate dielectric, is now less than 2 nm thick in state-of-the-art complementary metal–oxide–semiconductor devices, but it cannot be indefinitely scaled with current materials.[1] The material of choice for gate dielectrics has been thermally grown $SiO_2$ because of its excellent insulator properties, low defect densities, and its thermal stability. Unfortunately, the use of $SiO_2$ and $SiO_xN_y$ as gate dielectrics are reaching fundamental limits primarily due to high leakage currents across the dielectric.[2,3]

Instead of thinning the dielectric to obtain the necessary gate stack capacitance, insulating materials with a higher dielectric constant than $SiO_2$ can be used. A physically thicker high-*K* layer can be used to maintain low leakage current levels while attaining the necessary capacitance. A large number of alternative gate dielectric materials have been examined during the past few years including metal oxides such as $Ta_2O_5$, $TiO_2$, $HfO_2$, $ZrO_2$, $Y_2O_3$, $Al_2O_3$, and $La_2O_3$, as well as their silicates and aluminates.[4–11] Considerable attention has been given to $HfO_2$ due to its relatively high resistivity and dielectric constant (16–45).[12,13] Furthermore, $HfO_2$ appears to be thermally stable next to silicon at temperatures of up to $1000\,^{\circ}C$, and it is compatible with $n+$ polysilicon as the gate electrode material.[14]

The present article discusses the growth and characterization of high quality $HfO_2$ films using chemical vapor deposition (CVD) with hafnium-tetra-tert-butoxide [HTB, $Hf(C_4H_9O)_4$] as the precursor. Although physical vapor deposition (PVD) and atomic layer deposition (ALD, atomic layer CVD) have certain advantages in terms of control of interface and film homogeneity, if a simple CVD method can be devised to grow a high-*K* film with appropriate properties it would be easier to incorporate in a commercial industrial environment.

In conventional CVD processes, the deposition of metal oxides is usually accomplished by employing a precursor of the metal and an oxygen source such as water, ozone, or

[a)]Electronic mail: garf@rutchem.rutgers.edu

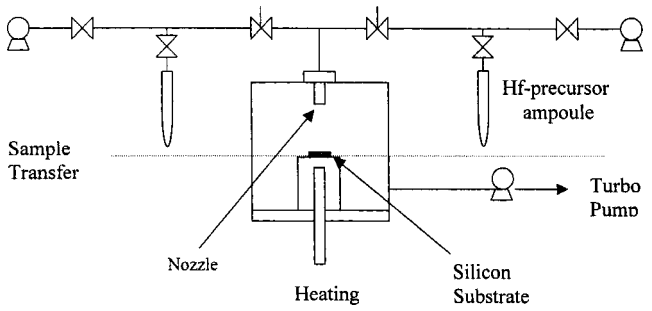


FIG. 1. CVD/ALD reactor designed and built at Rutgers and integrated with an UHV surface analysis system.

molecular oxygen. Unfortunately, many of the potential precursors have low vapor pressures, and thus have to be heated to obtain a practical flux through a reactor. Accurate control of the precursor, gas lines, and final injector (into the reactor) temperature become troublesome when higher temperatures are necessary to obtain a sufficient vapor pressure. Direct liquid injection, although useful for low vapor pressure precursors, has other disadvantages, including flow control problems and carrier decomposition. In some applications metal halides are chosen as the precursor, but delivery, contamination and reaction product (acid) etching can be problematic.[15] Some organometallics (e.g., $\beta$-diketonates and alkoxides) have been explored as precursors due to their high vapor pressure and low reactivity.[16,17] For the experiments discussed below, we used an alkoxide, hafnium-tetra-tert-butoxide (HTB), as the precursor.[18,19] HTB has some advantages compared to other hafnium molecular precursors. HTB has a relatively high vapor pressure ($\sim$0.07 Torr at 25 °C and $\sim$1 Torr at 65 °C) thus minimizing the heating of precursor and delivery lines. It does not decompose at temperatures below 225 °C, significantly reducing complications due to chamber wall or gas phase reactions. HTB can provide both the metal and the oxygen (required to grow a stoichiometric metal oxide) with the proper choice of reaction (decomposition) conditions, thus further reducing processing complexity. Under typical growth conditions it is possible that some oxygen also incorporates from background gases.

## II. EXPERIMENT

A laboratory-scale UHV-high pressure CVD/ALD growth chamber was designed, built, and interfaced to an UHV system, permitting thin films to be grown on Si samples ($\leqslant 20 \times 20$ mm) and analyzed. The HTB precursor was held in a small bubbler at a controlled temperature in a water bath. The precursor was introduced to the reactor through a heated gas line and nozzle (Fig. 1). The distance between the nozzle and the sample was $\sim$20 mm. The Si(100) substrates were placed on a sample holder which was heated by radiation from a halogen lamp located *ex vacuo* behind the sample holder. Sample temperature control from 25–450 °C was feasible, with heating rates of up to 5 °C/s. The base pressure in the growth chamber was $\leqslant 5\times10^{-7}$ Torr and was increased to the $10^{-3}$ Torr range during film growth (as measured by ion and Convectron gauges). The substrates were usually *p*-type Si(100) with a doping concentration of $1\times10^{15}$ cm$^{-3}$. A variety of starting surfaces have been explored: most of the work reported in this article used high-quality $\sim$11 Å commercial oxynitrides.

Compositional depth profiles were obtained using medium-energy ion scattering (MEIS),[20] a low energy ($\sim$100 keV in our case) high-resolution version of Rutherford backscattering spectroscopy (RBS). Depth resolution is much better than that of RBS due to the use of a high resolving power electrostatic analyzer[21] and because the ion energy loss (stopping power) for protons has its maximum in the range 50–100 keV.[22] One of the more straightforward properties to extract from the MEIS spectrum is the areal density. Depth profiles of elements are obtained from simulations of the backscattered ion energy distribution assuming the film's density is known or can be approximated.[23] Quantitative depth profiles for different species are extracted with a resolution as high as 3 Å in the near-surface region. Due to the statistical nature of the ion–solid interaction, the depth resolution deteriorates for deeper layers (ion straggling). For $HfO_2$ films the calculated absolute depth resolution at a depth of 30 Å is $\sim$8 Å, the relative changes in film (or interface layer) thickness at 30 Å determined with a precision better than 2 Å. MEIS data represent averages over a sample area (usually $\sim$0.1 mm$^2$), making it difficult to distinguish between near interface compositional gradients, and interface or surface roughness. Surface roughness of the CVD-grown films was determined independently by atomic force microscopy (AFM). Carbon contamination in the films was mostly located at the surface (this carbon could easily have been deposited during the *ex situ* transfer); bulk carbon levels were below the limit of MEIS sensitivity ($\leqslant$5%).

High resolution transmission electron microscopy (HRTEM) imaging was done using a JEOL JEM-4000 microscope operated at 400 keV to determine the crystal structure of the as-is and annealed $HfO_2$ films and to determine the interfacial thickness. The interfacial thickness determined from the HRTEM images was compared with the MEIS results. The cross-sectioned samples for HRTEM were prepared by mechanical polishing and subsequently thinned to electron transparency by argon–ion milling. Single wavelength ellipsometry measurements were performed using 632.8 nm light; refractive indices of 2.2 and 1.9 were used for $HfO_2$ and Si, respectively. A series of measurements was performed on each sample to obtain information on thickness variations. Capacitance–voltage ($C-V$) and current–voltage ($I-V$) curves were measured at 100 kHz on electron beam evaporated platinum dots with an area of $3.13\times10^{-4}$ cm$^2$. The leakage current densities were determined at 1 V past inversion V. $C-V$ and $I-V$ curves were measured at different locations on each sample; the numbers quoted below represent average values (the variation in numbers obtained was of the order of 5%). Finally we note that other experiments using photoemission and x-ray diffraction have been performed on these samples, and although not reported here, are consistent with the data presented below.

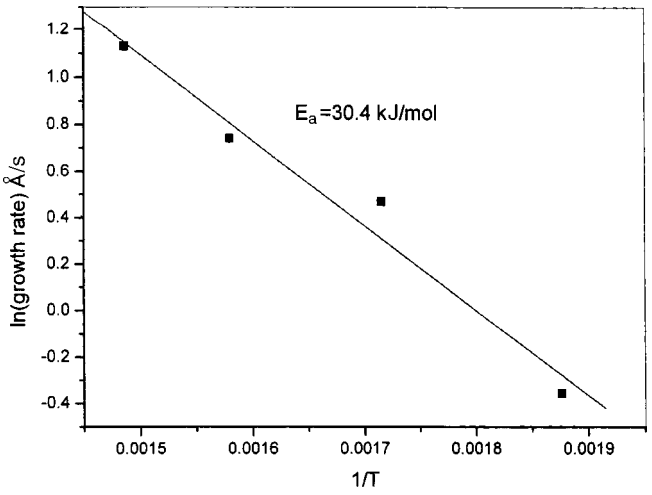


FIG. 2. Arrhenius plot of the logarithm of the $HfO_2$ film growth rate vs inverse temperature.

## III. RESULTS AND DISCUSSION

$HfO_2$ was deposited by introducing the pure precursor gas into the reactor in a temperature range of 250–450 °C at ~1 to 2 mTorr pressure. Figure 2 is an Arrhenius plot of the deposition rate (film thickness/time) as a function of temperature (ln rate versus 1/T), showing an activation energy of 30 kJ/mole. This relatively low value suggests that the rate-determining step occurs at the surface rather than in the gas phase. Following deposition, films were analyzed by AFM, MEIS, ellipsometry, HRTEM, and electrical methods ($C-V$ and $I-V$). As-deposited films were flat as determined by AFM, showing an rms roughness of $<2$ Å.

MEIS was used to examine the initial thin silicon oxynitride film on Si(100) that was used as a substrate for $HfO_2$ deposition. MEIS analysis showed the thickness of this film to be ~11 Å (estimated error ±1.5 Å) with nitrogen (total amount corresponding to $\sim 1.0\times10^{15}$ atoms/cm$^2$) located predominantly near the interface to the Si substrate.

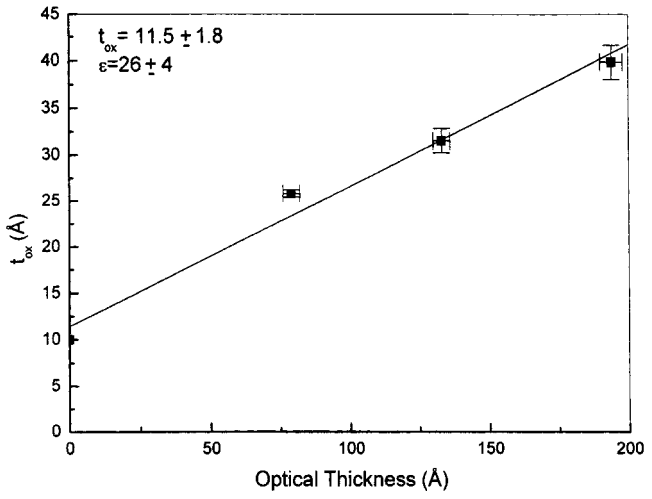


FIG. 3. Optical thickness (as determined from ellipsometry) plotted as a function of electrical thickness ($t_{ox}$).

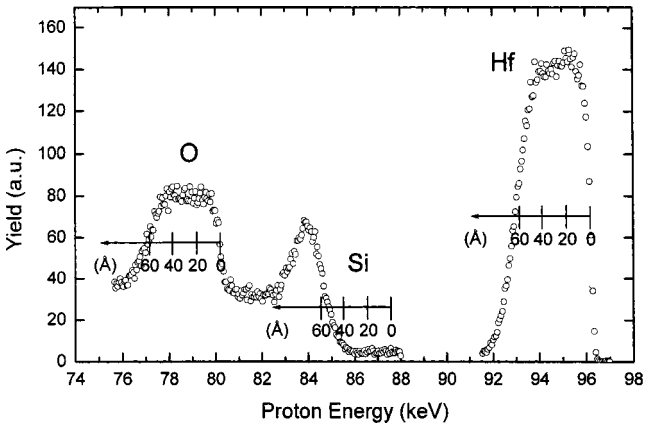


FIG. 4. MEIS spectra of an as-deposited $HfO_2/SiO_xN_y/Si$ sample.

In Fig. 3 we plot the thickness of a series of different thickness oxide films (grown on an oxynitride) in order to determine the effective dielectric constant of the $HfO_2$. The film thickness was determined both optically and electrically, and agreed quite well with the MEIS and HRTEM results. The electrical thickness (EOT) was determined by the capacitances at accumulation ($-2.5$ V). The dielectric constant of the $HfO_2$ was found to be $\sim 26\pm4$ by assuming a dielectric constant of 4 for the interfacial layer. The obtained value for the dielectric constant is in good agreement with the current literature consensus of $\sim 25\pm5$ for $HfO_2$ thin films. The intercept implies an interfacial oxide thickness (EOT) of 11.5±1.8 Å. (The errors associated with determination of the slope and intercept are calculated at 95% confidence level including the weighted error in $x$ and $y$ values.) The interfacial oxide thickness obtained is in agreement with the results of MEIS (11.0±1.5 Å).

Figure 4 shows a proton backscattering energy spectrum from the as-deposited $HfO_2$ film. The total amounts of Hf and O in the film were determined to be $1.5\times10^{16}$ and $3.6\times10^{16}$ atoms/cm$^2$, respectively. The position of the Si peak indicates that no or little Si diffusion toward the outer surface has occurred. The Si concentration in the film was found to be $<2\%$ of the Hf concentration. When using the known relative backscattering cross sections, the simulation yields a slightly O-rich $HfO_{2.17\pm0.06}$ film with a thickness of about 55 Å [Fig. 5(a)]. A silica/silicate layer was identified at the interface to the Si substrate with a thickness of about 14 Å. Due to the limited depth resolution of MEIS for deeper layers, details of the composition in the interface region can only be discerned with a depth resolution of ~8 Å. The MEIS profile may be interpreted as a graded Hf distribution in the interface region, as shown in Fig. 5(a). However, the MEIS data can also be modeled in a three layer (step function) model as 59 Å $HfO_2$, 9 Å $HfSiO_4$, little pure $SiO_2$ (Table I). These two different modeling procedures are both within the uncertainty of our MEIS modeling. The total amount of $SiO_2$ in the interfacial region can also be determined with higher accuracy from the directly measured areal densities of Si and O.

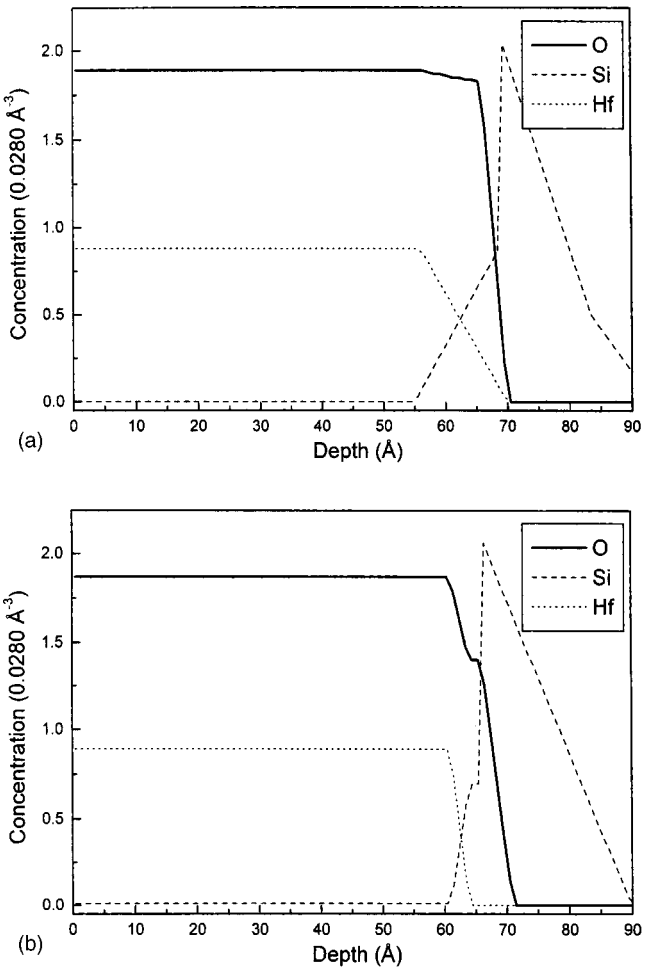


FIG. 5. (a) and (b) MEIS profile of as-deposited and annealed $HfO_2/SiO_xN_y/Si$ samples.

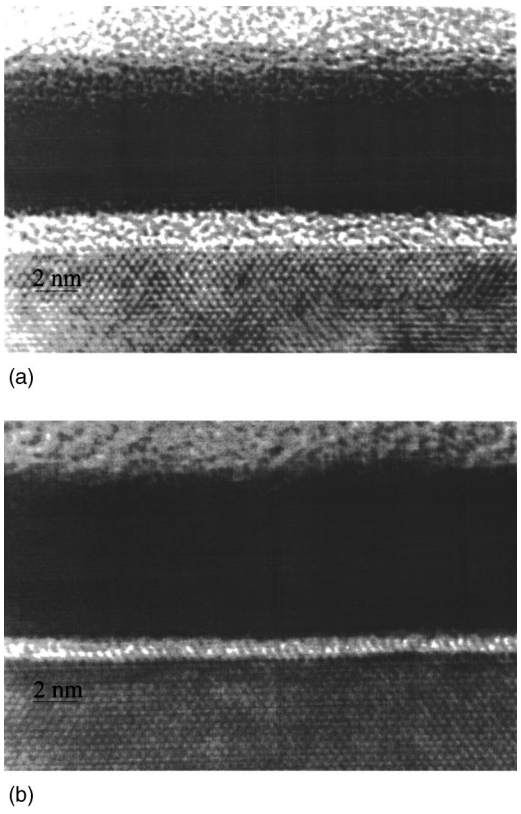


FIG. 6. (a) and (b) HRTEM images of as-deposited and annealed $HfO_2/SiO_xN_y/Si$ samples.

After vacuum annealing at 800 °C [Fig. 5(b)], the total amount of hafnium contained in the thin film remains constant (within the experimental accuracy given predominantly by variations in the film thickness). A $HfO_{2.10\pm0.06}$ film with a thickness of 61 Å is observed. Again, the Si concentration in the film was found to be below the detection limit, implying that there is no Si diffusion into the film. An ~5 Å thick interfacial layer between the $HfO_2$ and the Si substrate is observed.

Some changes, however, can be observed in the MEIS spectra of the annealed sample. The high-energy edge of the hafnium peak becomes somewhat more sharp, due in part to the loss of surface carbon ($<1\times10^{15}$ atoms/cm$^2$, CH-species on the surface from residual hydrocarbons in the atmosphere). The low energy edge of the hafnium peak in the MEIS spectrum (and the high energy edge of the silicon peak) also sharpens even more than the high energy Hf edge [Fig. 5(a)], indicating a sharper interface between the $HfO_2$ and the underlying $SiO_2$ structure. The interfacial region seems to consist of an almost pure $SiO_2$ film with a thickness of 5 Å.

In spite of the limitations in depth resolution of MEIS, the Hf distribution for this annealed sample cannot be interpreted as a uniformly graded Hf distribution extending to the Si substrate. Modeling the Hf distribution as a pair of step functions yields a better fit, resulting in a film structure of 62 Å $HfO_2$, almost no $HfSiO_4$, and a pure 5 Å $SiO_2$ film at the interface.

Figure 6(a) shows an HRTEM image obtained from a cross section of an as-deposited $HfO_2$ film. The substrate lattice is well-resolved providing an internal reference length [the Si(111) lattice spacing of 3.13 Å] for measuring the oxide thickness. The primary uncertainty associated with thickness determination in this HRTEM measurement lies in the assignment of the film surfaces and interfaces. This error can be as large as ±4 Å depending on the specific film (it increases for a rough film) and HRTEM imaging conditions.

TABLE I. Electrical results (as determined from $C-V$ and $I-V$ plots) on as-deposited and annealed samples.

| Sample | $Tqm$ (Å) | $V_{\text{flatband}}$ (V) | Hysteresis (V) | $J$ (A/cm$^2$) |
|---|---|---|---|---|
| as-is | 18.6±0.9 | 0.80±0.01 | 0.17±0.01 | $7.4\times10^{-8}$ |
| annealed | 21.9±0.3 | 0.37±0.13 | 0.14±0.03 | $2.6\times10^{-5}$ |

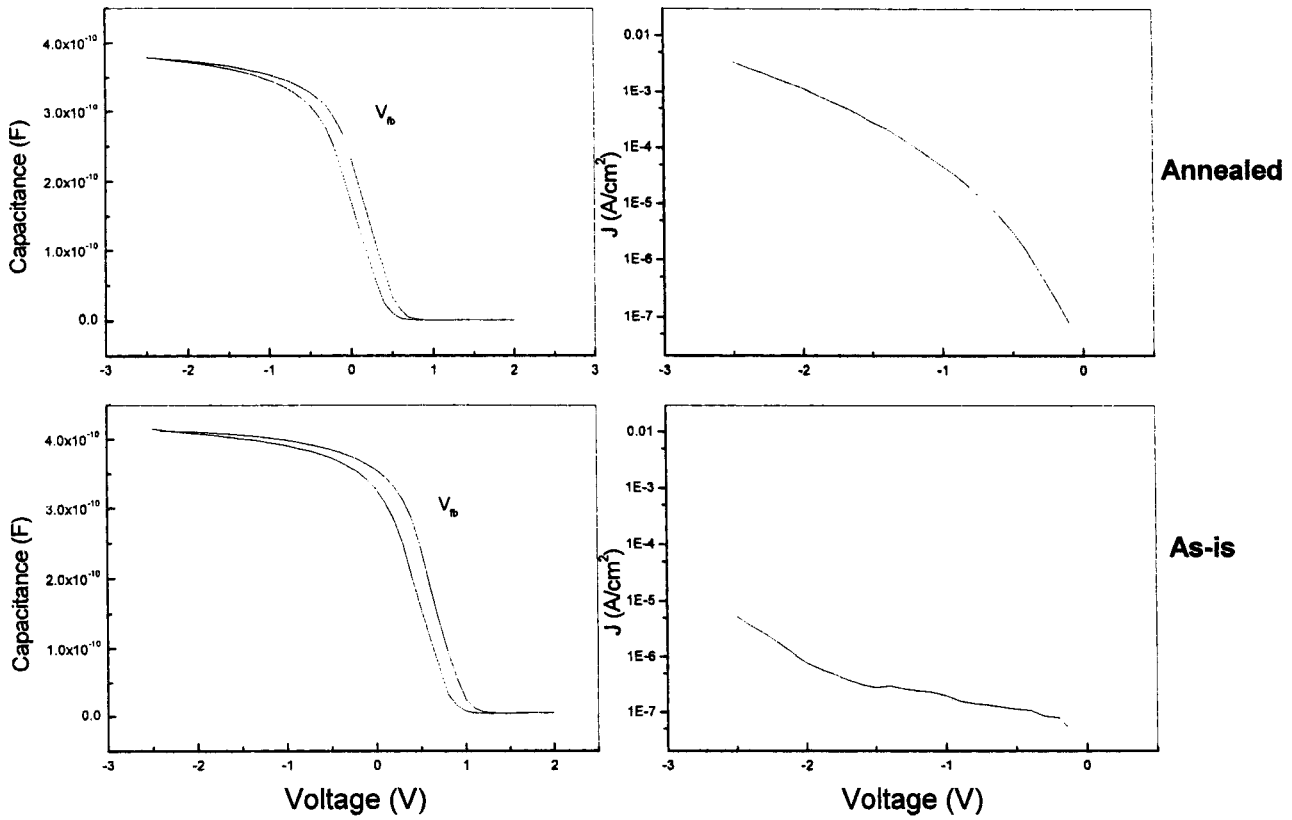


FIG. 7. Capacitance–voltage and current–voltage diagrams for as-deposited and annealed $HfO_2/SiO_xN_y/Si$ samples.

The thickness of the interfacial layer and $HfO_2$ film are found to be $16\pm4$ and $65\pm4$ Å, respectively, for the as-deposited film. The HRTEM of the $HfO_2$ films annealed in vacuum at 800 °C is shown in Fig. 6(b) where the interfacial layer (thickness) is $9\pm3$ Å and the $HfO_2$ film is $67\pm3$ Å. For the as-deposited sample, HRTEM indicates the presence of a few nanometer-sized crystallites; nevertheless, the film appeared to be predominantly amorphous. After annealing, however, the metal oxide film became polycrystalline.

Results from electrical measurements of the films are given in Fig. 7 and Table I. The (electrical) equivalent oxide thicknesses (EOTs) were determined from the capacitance in accumulation at $-2.5$ V and were corrected for quantum mechanical effects. The electrical thickness was found to be $18.6\pm0.6$ and $21.9\pm0.3$ Å for the as-deposited and annealed samples, respectively. The increase in electrical thickness after annealing ($3.3\pm0.9$ Å) may be attributed to an increase in interfacial oxide thickness as a result of phase segregation between $HfO_2$ and $SiO_2$ as evidenced by MEIS measurements. Film EOTs as thin as 12 Å (data not shown) with leakage currents $<10^{-6}$ A/cm$^2$ were observed when the starting oxynitride was 8 Å and the overlayer was 25 Å $HfO_2$.

The flatband voltage for an ideal capacitor with a Pt electrode ($\Phi_B=5.65$ eV)[24] and $p$-Si ($1\times10^{15}$ cm$^{-3}$) substrate should be 0.65 V; we measured 0.80 V for our as-deposited samples, indicating negative charge in the film. The flatband voltage shift $\Delta V_{FB}$ (the difference in the flatband voltage from that expected for an ideal capacitor) for the as-deposited samples was $\sim150$ mV. The flatband voltage shifts for sputtered ultrathin $HfO_2$ films measured using Pt electrodes were reported as $\sim600$ and $\sim-300$ mV.[16,17] After 800 °C anneal for 5 min, the flatband voltage was 0.37 V, indicating positive charge. The flatband voltage shift, $\Delta V_{FB}$, in this case was $-280$ mV. This change in the flatband voltage shift cannot be fully explained by a change in total oxide capacitance. The observed changes in the interfacial layer thickness and EOT value (as measured by MEIS and $C-V$, respectively) upon annealing may contribute to the measured shift in $\Delta V_{FB}$, but further investigation will be required. It does appear, however, that there is significantly less negative charge in the gate stack after anneal. The hysteresis remained nearly constant after annealing to 800 °C for 5 min. These results are summarized in Table I. On the other hand, the leakage current density increased significantly, possibly a result of increased nanocrystallinity of the film, which is evident from a comparison of the corresponding HRTEM micrographs (Fig. 6).

## IV. SUMMARY

In this article we have presented new MEIS and HRTEM results demonstrating that high-quality, ultrathin films of $HfO_2$ can be deposited on Si(100) using a simple HTB based thermal CVD process. The measurements using various techniques agree to within $\sim15\%$ (e.g., for the film thickness);

they present a generally consistent picture of film structure and composition. The films display physical and electrical properties appropriate for use as a gate oxide. The as-deposited films were slightly oxygen-rich despite the fact that no additional oxygen was introduced during deposition. Films were stable with respect to reaction with the substrate. Promising electrical properties were obtained when the $HfO_2$ film was grown on $SiO_xN_y$. Some initial intermixing between the $SiO_2$ and $HfO_2$ layers is implied by the MEIS depth profiles (and also indicated by capacitance measurements); this intermixed region sharpens up as the films are annealed to 800 °C. After annealing at 800 °C, the films were mostly crystalline in structure, accompanied by an increase in leakage current. Films with an EOT as thin as 12 Å were produced using this CVD technique, while still exhibiting low leakage currents. Current work is directed towards further understanding the differences in the properties of films produced by CVD, ALD, and PVD-based methods.

## ACKNOWLEDGMENTS

The authors would like to acknowledge the Semiconductor Research Corporation and the National Science Foundation for financial support of this work. We also thank and Dr. Marty Green (Agere Systems/Bell Labs) and Dr. Evgeni Gusev (IBM-YTH) for their help and insight.

[1]International Technology Roadmap for Semiconductors (2000), International Sematech (Austin).
[2]L. Feldman, E. P. Gusev, and E. Garfunkel, in *Fundamental Aspects of Ultrathin Dielectrics on Si-based Devices*, edited by E. Garfunkel, E. P. Gusev, and A. Y. Vul' (Kluwer, Dordrecht, 1998), p. 1.
[3]D. A. Buchanan, IBM J. Res. Dev. **43**, 245 (1999).
[4]G. D. Wilk, R. M. Wallace, and J. M. Anthony, J. Appl. Phys. **89**, 5243 (2001).
[5]S. A. Campbell, D. C. Gilmer, X. C. Wang, M. T. Hsieh, H. S. Kim, W. Gladfelter, and J. Yan, IEEE Trans. Electron Devices **44**, 104 (1997).
[6]G. B. Alers, D. J. Werder, Y. Chabal, H. C. Lu, E. P. Gusev, E. Garfunkel, T. Gustafsson, and R. Urdahl, Opt. Lett. **73**, 1517 (1998).
[7]A. I. Kingon, J.-P. Maria, and S. K. Streiffer, Nature (London) **406**, 1032 (2000).
[8]B. H. Lee, L. Kang, W.-J. Qi, R. Nieh, Y. Jeon, K. Onishi, and J. C. Lee, Tech. Dig. - Int. Electron Devices Meet. **133**, (1999).
[9]M. Copel, M. Gribelyuk, and E. Gusev, Appl. Phys. Lett. **76**, 436 (2000).
[10]G. Lucovsky and J. C. Phillips, Microelectron. Eng. **48**, 291 (1999).
[11]B. W. Busch, W. H. Schulte, E. Garfunkel, T. Gustafsson, W. Qi, J. Nieh, and J. Lee, Phys. Rev. B **62**, R13290 (2000).
[12]C. T. Hsu, Y. K. Su, and M. Yokoyama, Jpn. J. Appl. Phys., Part 1 **31**, 2501 (1992).
[13]K. Kukli, J. Aarik, A. Aidla, H. Siimon, M. Ritala, and M. Leskela, Appl. Surf. Sci. **112**, 236 (1997).
[14]L. Kang, K. Onishi, Y. Jeon, B. H. Lee, C. Kang, W.-J. Qi, R. Nieh, S. Gopalan, R. Choi, and J. C. Lee, Tech. Dig. - Int. Electron Devices Meet. **35**, (2000).
[15]A. C. Jones, T. J. Leedham, P. J. Wright, M. J. Crosbie, K. A. Fleeting, D. J. Otway, P. O'Brien, and M. E. Pemble, J. Mater. Chem. **8**, 1773 (1998).
[16]J. C. Rey, L. Y. Cheng, J. P. McVittie, and K. C. Saraswat, J. Vac. Sci. Technol. A **9**, 1083 (1991).
[17]A. Burke, G. Braeckelmann, D. Manger, E. Eisenbraun, A. E. Kaloyeros, J. P. McVittie, J. Han, D. Bang, J. F. Loan, and J. J. Sullivan, J. Appl. Phys. **82**, 4651 (1997).
[18]M. A. Cameron and S. George, Thin Solid Films **348**, 90 (1999).
[19]T. S. Jeon, J. M. White, and D. L. Kwong, Appl. Phys. Lett. **78**, 368 (2001).
[20]J. F. van der Veen, Surf. Sci. Rep. **5**, 199 (1985).
[21]R. M. Tromp, M. Copel, M. C. Reuter, M. H. v. Hoegen, J. Speidell, and R. Koudijs, Rev. Sci. Instrum. **62**, 2679 (1991).
[22]J. F. Ziegler and J. P. Biersach, *SRIM - The Stopping Range of Ions in Matter, Ver. 9*, (IBM Research, Yorktown Heights, NY, 1998).
[23]E. P. Gusev, H. C. Lu, T. Gustafsson, and E. Garfunkel, Phys. Rev. B **52**, 1759 (1995).
[24]*CRC Handbook of Chemistry and Physics* (Chemical Rubber Corp., Boca Raton, FL, 1990).